Available online at www.sciencedirect.com

ScienceDirect

Ceramics International 39 (2013) 9063–9070

CERAMICS INTERNATIONAL

www.elsevier.com/locate/ceramint

# Mullite-based refractory castable engineering for the petrochemical industry

A.P. Luz[a,*], A.B. Silva Neto[a], T. Santos Jr.[a], J. Medeiros[b], V.C. Pandolfelli[a]

[a]Federal University of São Carlos (UFSCar), Materials Engineering Department, Rodovia Washington Luiz, km 235, São Carlos, SP 13565-905, Brazil
[b]Petrobras, Research and Development Center (CENPES), Rio de Janeiro, RJ 21941-915, Brazil

Received 21 April 2013; received in revised form 29 April 2013; accepted 2 May 2013
Available online 16 May 2013

## Abstract

Refractory castables used in fluid catalytic converter (FCC) risers should present suitable particle erosion and thermal shock resistances at temperatures below 900 °C. Considering that calcium aluminate cement (CAC)-bonded refractories usually start their densification above 1200 °C, the use of sintering additives to induce faster densification is a promising technological alternative. Therefore, this work addresses the evaluation of mullite-based castables containing a boron-based sintering additive and CAC and/or hydratable alumina as the binder sources. Hot elastic modulus, cyclical thermal shock, hot modulus of rupture and cold erosion resistance measurements were carried out to evaluate the compositions. According to the attained results, adding 1.5 wt% of the evaluated sintering additive to the designed castables led to a remarkable increase of the hot modulus of rupture (maximum of 40.4 MPa at 800 °C for the CAC-containing refractory) and high erosion resistance (1.5–2.9 $cm^3$) after pre-firing at 800 °C for 5 h. Moreover, the combination of CAC and hydratable alumina gave rise to an improved refractory (M–2CAC–2HA–S) showing a transient liquid formation at an increased temperature, high thermal shock resistance (no $E$ decay after 8 thermal cycles, $\Delta T = 800$ °C) and high mechanical strength at 800 °C and 1000 °C.

*Keywords:* D. Mullite; Binder; Refractory castables; Sintering additive

## 1. Introduction

The growing demand for refractory castables with designed properties has brought about continuous technological development involving the simultaneous understanding of particle size distribution, the use of additives (inducing better dispersion of particles in aqueous medium [1,2], speeding up the compositions' densification [3,4], etc.) and the binders' performance [5–8].

Refractory castables applied in risers for petrochemical fluid catalytic converters (FCC, Fig. 1) are commonly exposed to temperature fluctuations and mainly to high speed catalyzer particles [9]. Therefore, thermal shock and particle erosion resistances are some of the main requirements for this application. Additionally, these castables should present optimized properties around 800 °C but, depending on the working conditions, some regions of the refractory lining can reach peaks of temperature close to 1200 °C. Hence, as most commercial cement-bonded castables show densification only at temperatures above 1200 °C, a different composition approach should be designed to match the refractory's performance requirements for the petrochemical industries [3].

Considering the increasing interest in the development of refractories presenting optimized hot mechanical strength in the range of 800–1200 °C, as well as the necessity for using less dense compositions due to the risers´ geometry (the height/diameter ratio usually ranges between 30 and 50 times [9]), there is a continuous motivation for the design of novel castable formulations to better fulfill those needs, maintaining high erosion and thermal shock resistances.

In order to attain refractories with enhanced properties at high temperatures, calcia-free binders [i.e., hydratable alumina (HA), colloidal silica and colloidal alumina] containing castables have been developed [3,10,11]. For densification at temperatures close to 800 °C, previous studies [3,4] pointed out that an interesting alternative based on using sintering

---

[*]Corresponding author. Tel.: +55 16 33518253; fax: +55 16 33615404.
*E-mail addresses:* anapaula.light@gmail.com (A.P. Luz), vicpando@ufscar.br (V.C. Pandolfelli).

0272-8842/$ - see front matter © 2013 Elsevier Ltd and Techna Group S.r.l. All rights reserved.
http://dx.doi.org/10.1016/j.ceramint.2013.05.001

additives led to liquid formation and, consequently, faster densification of refractories containing CAC or colloidal binders (silica or alumina). Nevertheless, selecting these additives should be tailored, as a liquid phase can result in refractoriness drawbacks. High alumina and mullite compositions containing calcium aluminate cement and 2 wt% of a boron-based sintering additive, for instance, presented remarkable hot mechanical strength, thermal shock and erosion resistances at 800 °C. Nevertheless, above this temperature, the presence of a liquid phase resulted in a significant decrease of the hot modulus of rupture of those materials [4].

Various studies have shown that HA bonded castables present high refractoriness. However, similar to CAC, it does not provide good mechanical strengths at temperatures below 1200 °C [11–14]. Based on these aspects, the aim of this work was to evaluate mullite refractory castables designed for petrochemical applications containing a boron-based sintering additive and CAC and/or hydratable alumina (HA) as the binder sources. Hot elastic modulus tests (using the bar resonance method) were carried out in order to follow the phase transformations in dried (110 °C for 24 h) and fired (1000 °C for 5 h) samples with and without a holding time of 5 h at 1000 °C. Furthermore, apparent porosity, hot modulus of rupture, erosion resistance and XRD quantitative analysis of the crystalline phases contained in the samples were also performed for a better understanding of the refractories' behavior.

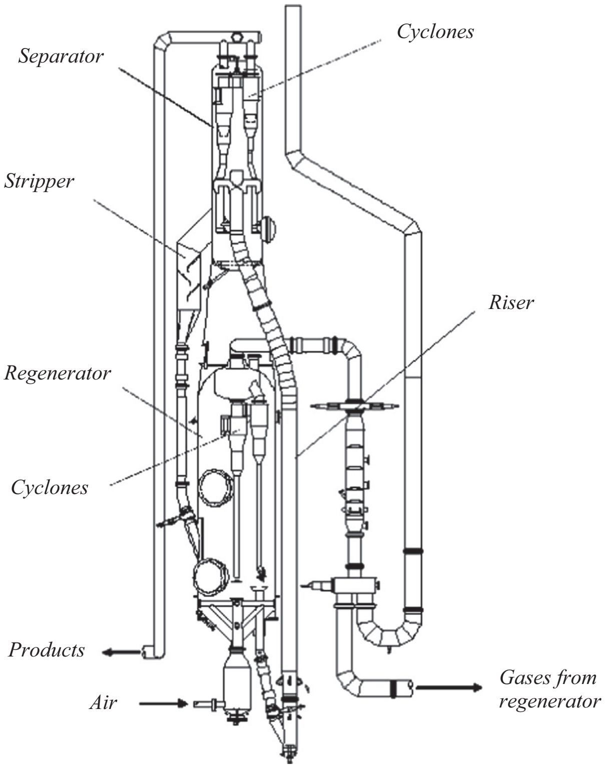

Fig. 1. Typical features of a petrochemical fluid catalytic converter unit — FCCU [9].

## 2. Experimental

Four self-flowing mullite based castables were designed according to Alfred's packing model ($q$=0.21) [15]. The compositions comprised coarse synthetic mullite (Mulcoa 70, $Al_2O_3$ = 69 wt% and $SiO_2$ = 27 wt%, Treibacher, USA) as aggregates, calcium aluminate cement (CAC, Secar 71, Kerneos, France) or hydratable alumina (HA, Alphabond 300, Almatis, USA) as binders, reactive aluminas (CL370C and CT3000SG, Almatis, USA) and a boron-based additive ($d < 45$ μm, S, under patent application) in order to speed up the densification of the refractories in the usual temperatures for petrochemical applications (~800 °C for FCC risers) [3,4]. A sintering additive-free composition (M–4CAC) was also prepared and tested as a reference. Table 1 presents further details of the formulated castables.

The castable dispersion was carried out by adding 0.2 wt% of a polycarboxylate based dispersant (Basf, Germany), leading to 5.8–6.2 wt% water content for suitable shaping (free-flow values = 62–68%). The compositions were prepared in a rheometer especially developed for refractory castables, by adding the mixing water using a two-step procedure [16].

After the mixing step, prismatic samples (150 mm × 25 mm × 25 mm) were molded, cured at 50 °C for 24 h in a humid environment (relative humidity = 80% for castables containing CAC: M–4CAC, M–4CAC–S and M–2CAC–2HA–S, whereas the M–4HA–S samples were kept in a chamber without humidity control), dried at 110 °C for another 24 h, followed by firing at 600, 800, 1000 and 1200 °C for 5 h in electrical furnace (Lindberg Blue, Lindberg Corporation, USA).

Hot modulus of rupture (HMOR) tests were carried out at 600 °C, 800 °C, 1000 °C and 1200 °C (using samples pre-fired for 5 h at the same testing temperature) in HBTS 422 equipment (3-point bending test, Netzsch, Germany) based on the ASTM C583-8 standard. The apparent porosity of the fired samples was measured by the Archimedes method (ASTM C380-00), using kerosene as the immersion liquid. Cold erosion resistance measurements were also performed (using samples fired at 600, 800 and 1000 °C for 5 h), following the ASTM C704 standard (1 kg of no. 36 grit silicon carbide to erode samples 10 cm × 10 cm × 2.5 cm thick, leading to a weight loss that was converted to a volumetric one).

Table 1
General information of the castable compositions.

| Raw materials | Compositions (wt%) | | | |
|---|---|---|---|---|
| | M–CAC | M–4CAC–S | M–4HA–S | M–2CAC–2HA–S |
| Mullite aggregates ($d \leq 3$ mm) | 84.5 | 83.5 | 85.5 | 83.5 |
| Reactive aluminas | 11.5 | 11.0 | 9.0 | 11.0 |
| Calcium aluminate cement | 4.0 | 4.0 | – | 2.0 |
| Hydratable alumina | – | – | 4.0 | 2.0 |
| Sintering additive ($d \leq 45$ μm) | – | 1.5 | 1.5 | 1.5 |

Some prismatic samples were ground ($dp < 45$ μm) in a tungsten carbide mill (AMEF, model AMP1-M, Brazil) and analyzed using the X ray diffraction technique (Bruker equipment, model D8 Focus, Germany, with CuKα radiation [$\lambda = 1.5418$ Å] and nickel filter, using 40 mA, 40 mV, and scanning step = 0.02 for 2$\theta$ between 4 and 80°). The Rietveld method (Topas 4.2 software, Bruker) was used to analyze the XRD results in order to evaluate the amount of phases comprising the fired samples.

Pre-fired refractories (800 °C for 5 h) were subjected to a total of 10 thermal shock cycles (ASTM C1171-91). The samples were placed into a furnace chamber previously heated at 825 °C and kept at this temperature for 15 min. After that, they were withdrawn and cooled in air for another 15 min, leading to thermal gradients of roughly 800 °C. This procedure was considered as one full cycle. The damage caused by the thermal changes was evaluated by the elastic modulus measurements at room temperature (bar resonance, ASTM C 1198-91) as a function of the thermal cycles (0, 2, 4, 6 and 8).

Hot elastic modulus tests were also carried out in the prismatic samples after previous processing steps (curing at 50 °C for 24 h and drying at 110 °C for 24 h, or after pre-firing at 1000 °C/5 h). The bar resonance method (which is based on sample excitation and detecting the correspondent vibration spectrum using piezoelectric transducers [17]) was also used in these analyses. The measurements were conducted in the 30–1000 °C range with a heating rate of 2 °C min$^{-1}$, with or without a holding time of 5 h at the maximum temperature.

## 3. Results and discussion

Fig. 2 shows the hot modulus of rupture (HMOR) and apparent porosity results of the pre-fired samples.

Comparing the M–4CAC and M–4CAC–S performance, lower mechanical strength values were attained for the former (additive-free refractory) between 600 and 1000 °C, which highlights the late densification of this material. Conversely, the addition of the boron-based sintering additive (S) to the other compositions has led to a marked increase in the samples ´ mechanical strength mainly at 800 °C and 1000 °C (Fig. 2a). HA containing compositions achieved their highest mechanical strength at 1000 °C, whereas castable M–4CAC–S showed a continuous decrease of HMOR values above 800 °C. Such behavior indicates the lower refractoriness of the cement-bonded material especially after adding the sintering additive, resulting in the formation of a $B_2O_3$-containing liquid phase in the refractory structure [3].

Few changes in the apparent porosity levels of the M–4CAC samples were detected in the evaluated temperature range (Fig. 2b). On the other hand, the other compositions presented a drop of the volume pore content mainly above 600 °C. It must be pointed out that even with the decrease of the apparent porosity, the M–4CAC–S, M–4HA–S and M–2CAC–2HA–S castables still showed a marked decay of the hot mechanical strength, which most likely is related to the action of the sintering additive, inducing the formation of a liquid phase at high temperature.

In order to better explain the castables' behavior, it is necessary to understand the phase transformations taking place in the samples structure. Nevertheless, there are some experimental difficulties for the evaluation of boron-containing systems, as the reactions may include $B_2O_3$ volatilization at high temperatures, the high viscosity of borosilicate melts inhibits their tendency for crystallization and such light element (B) is difficult to be detected by EPMA [18]. Moreover, the $CaO–Al_2O_3–B_2O_3$ and $CaO–Al_2O_3–SiO_2–B_2O_3$ systems are not well known based on the experimental point of view. The only available $CaO–Al_2O_3–B_2O_3$ phase diagram (Fig. 3a) presented in the literature was studied by Schaefer and Kuzel [19]. According to their analyses, two ternary compounds $CaO \cdot Al_2O_3 \cdot B_2O_3$ (CAB) and $2CaO \cdot Al_2O_3 \cdot B_2O_3$ ($C_2AB$) can be formed and they should melt incongruently at 1015 °C and 800 °C, as shown in Eqs. (1) and (2), giving rise to solid and liquid phases.

$$CaO{\cdot}Al_2O_3{\cdot}B_2O_3 \rightarrow 9Al_2O_3{\cdot}2B_2O_3 + L \tag{1}$$

$$2CaO{\cdot}Al_2O_3{\cdot}B_2O_3 \rightarrow CaO{\cdot}2Al_2O_3 + L \tag{2}$$

Based on the quantitative XRD analysis of the M–4CAC–S castable fired at 600 °C, 800 °C, 1000 °C and 1200 °C for 5 h (Fig. 4a), the main identified crystalline phases were mullite, corundum, $2Al_2O_3 \cdot B_2O_3$ ($Al_4B_2O_9$ or $A_2B$) and $9Al_2O_3 \cdot 2B_2O_3$ ($Al_{18}B_4O_{33}$ or $A_9B_2$).

It is believed that those aluminum-borates should be formed at high temperatures most likely due to the interaction between the reactive alumina and mullite fine grains with the sintering additive in the samples' matrix. Minor contents of $SiO_2$, $CaAl_2Si_2O_8$ (anorthite) and CAB were also detected. Additionally, as reported in the proposed phase equilibrium diagrams in the $Al_2O_3–B_2O_3$ system (Fig. 5) [21–23], $A_2B$ and $A_9B_2$ can be found accompanied by a liquid phase above 470 °C. Hence, the formed boron-based liquid might be the reason for spoiling the M–4CAC–S mechanical performance mainly at high temperatures.

Regarding the M–4HA–S composition, the absence of CaO in this castable allows a direct comparison of the attained phase evolution (XRD results—Fig. 4b) and the ternary $Al_2O_3–SiO_2–B_2O_3$ phase diagram (Fig. 3b). Additionally, the main ternary invariant reactions that can take place in this system throughout the heating stage are shown in Table 2.

According to those reactions, the liquid phase itself or its interaction with other components may generate new solid phases such as aluminum-borates ($A_2B$ or $A_9B_2$) and silica or mullite. These transformations indicate that even when a boron-containing liquid was formed in the hydratable alumina-bonded castables (M–4HA–S and M–2CAC–2HA–S), this phase is consumed, leading to the formation of other solid components, which explains the higher mechanical strength attained at 1000 and 1200 °C for these refractories (Fig. 2a). As shown in Fig. 4b and c, high contents of $A_2B$ and $A_9B_2$, as well as other aluminum-borates [$AlBO_3$, $Al_5(BO_3)_6$] were identified in the fired M–4HA–S and M–2CAC–2HA–S samples.

Nevertheless, the lower HMOR values attained for the M–4HA–S samples at 800 °C should be related to the

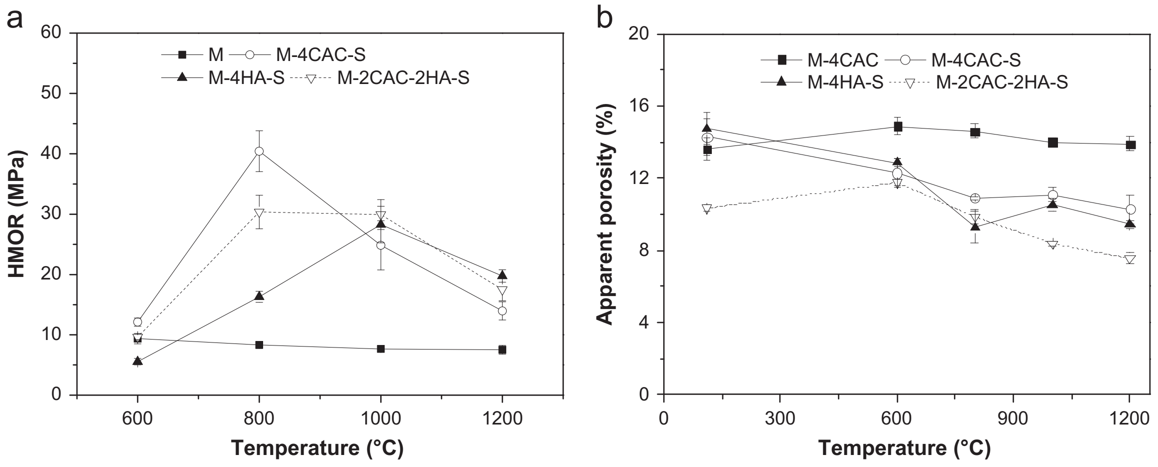

Fig. 2. (a) Hot modulus of rupture (HMOR) and (b) apparent porosity of the evaluated castables after pre-firing treatment at 600, 800, 1000 and 1200 °C for 5 h. (The connecting lines were drawn only to guide the eyes).

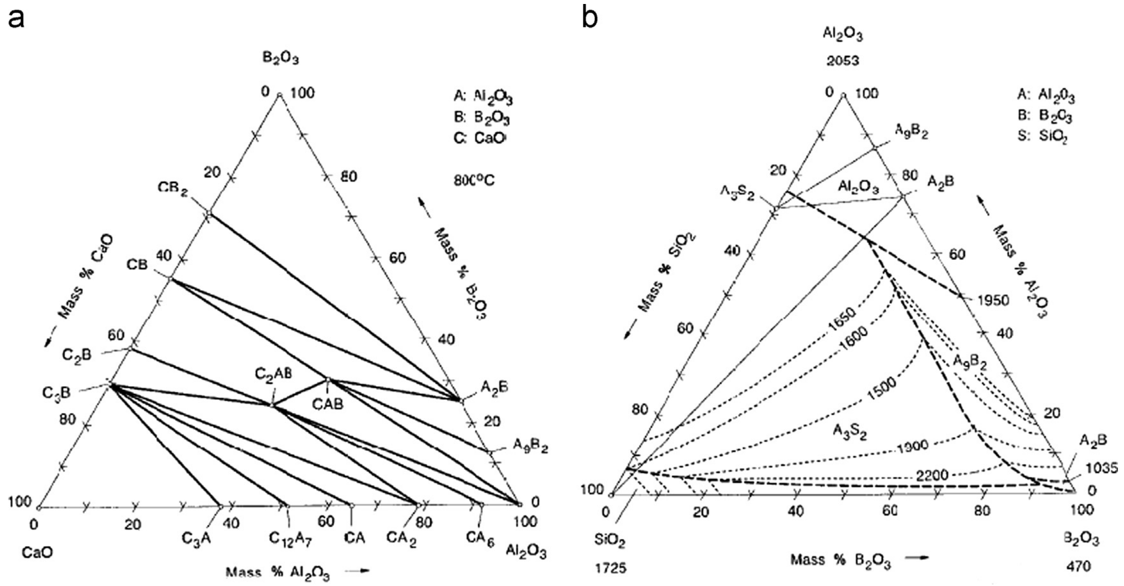

Fig. 3. (a) Isothermal section of the $Al_2O_3$–$B_2O_3$–CaO system at 800 °C, and (b) liquidus surface in the $Al_2O_3$–$B_2O_3$–$SiO_2$ system [20].

intermediate phases [$AlBO_3$, $B_2O_3$ and $Al_5(BO_3)O_6$] still present in the castable microstructure after the pre-firing treatment. With the increase of the firing temperature, those components should be consumed and induce the generation of a larger amount of the $A_2B$, $A_9B_2$ phases at 1000 and 1200 °C (as shown in Fig. 4b), improving the castable performance.

Concerning the cold erosion resistance of the compositions, the faster densification of the castables (due to the addition of the sintering additive) resulted in very low eroded volumes for the M–4CAC–S, M–4HA–S and M–2CAC–2HA–S samples fired at 800 and 1000 °C for 5 h (Table 3).

Aiming to evaluate the densification effect induced by the sintering additive and the binders role in the refractories properties, *in situ E* analyses were also carried out up to 1000 °C for dried (110 °C for 24 h) and pre-fired (1000 °C/5 h) samples. Fig. 6 shows the elastic modulus evolution attained during three thermal cycles for the four designed compositions. An additional analysis of the first heating/cooling cycle of the pre-fired materials was also performed.

Although the CAC-bonded compositions presented higher initial *E* values (varying from 48 to 68 GPa), they showed the usual decrease of this property between 200 and 400 °C (1st heating cycle) due to the cement hydrates decomposition [2]. No major changes in the attained curves of the additive-free samples above 400 °C, during cooling and also along the 2nd and 3rd cycles were detected (Fig. 6a), indicating that no densification took place up to 1000 °C. Moreover, the result for the pre-fired M–4CAC castable showed a similar behavior, as an overlap of the curves can be observed.

On the other hand, samples M–4CAC–S and M–2CAC–2HA–S (Fig. 6b and d) presented an elastic modulus increase from 600 °C up to 1000 °C, mainly due to the samples´

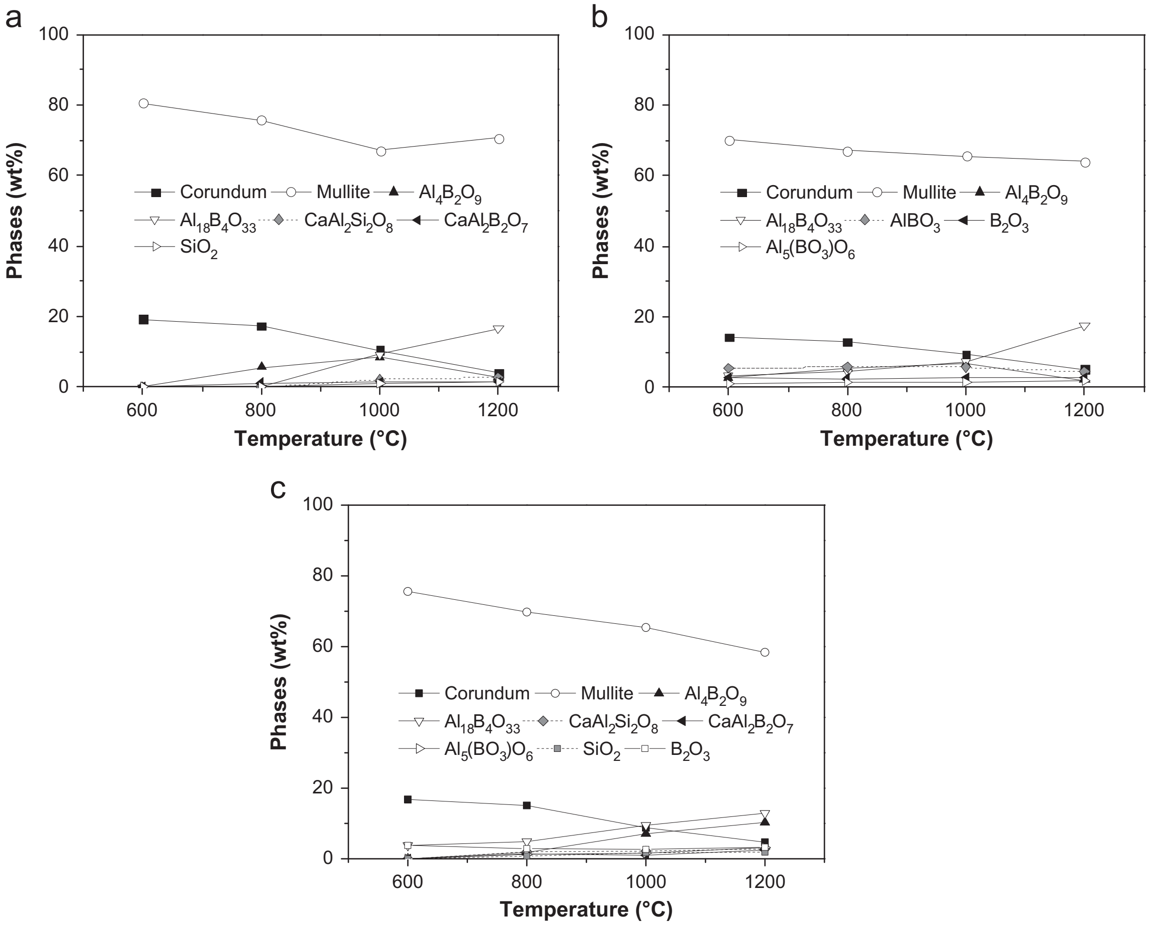

Fig. 4. Phase evolution for the (a) M–4CAC–S, (b) M–4HA–S and (c) M–2CAC–2HA–S samples after firing at different temperatures for 5 h. The phase contents were obtained by XRD quantitative measurements (Rietveld method).

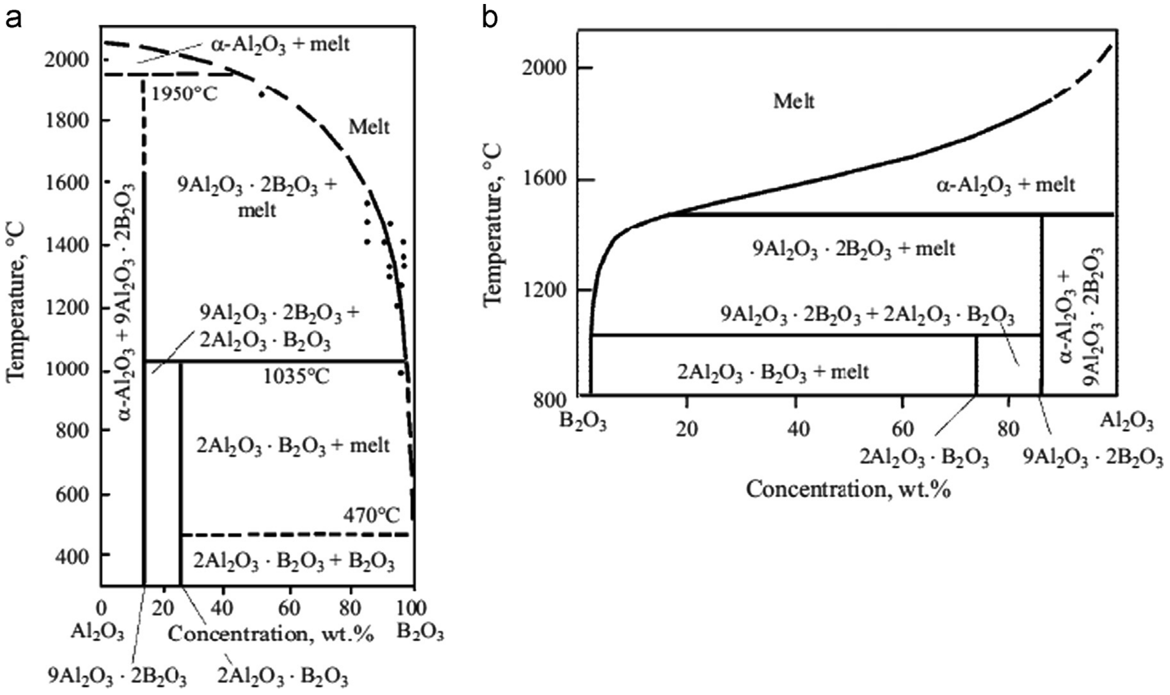

Fig. 5. $Al_2O_3$–$B_2O_3$ phase diagrams reported in the literature by (a) Kim et al. [22] and (b) Gielisse et al. [23].

Table 2
Ternary invariant reactions in the $Al_2O_3$–$B_2O_3$–$SiO_2$ system [18].

| Temperature (°C) | Invariant reactions | Composition ($Al_2O_3$, $B_2O_3$, and $SiO_2$) (wt%) |
|---|---|---|
| 1770 | $Al_2O_3 + L \rightarrow Al_{18}B_4O_{33}$ + mullite | 69.4, 23.0, and 7.7 |
| 1128 | $Al_{18}B_4O_{33} + L \rightarrow Al_4B_2O_9$ + mullite | 1.8, 9.0, and 8.6 |
| 810 | Mullite + $L \rightarrow Al_4B_2O_9 + SiO_2$ (quartz) | 0.1, 66.3, and 33.6 |
| 438 | $L \rightarrow Al_4B_2O_9 + SiO_2$ (quartz) + $B_2O_3$ | 0, 93.0, and 7.0 |

Table 3
Eroded volume of the pre-fired castables as a function of the temperature.

| Temperatura (°C) | Eroded volume ($cm^3$) | | | |
|---|---|---|---|---|
| | M–4CAC | M–4CAC–S | M–4HA–S | M–2CAC–2HA-S |
| 600 | $10.3 \pm 0.8$ | $6.6 \pm 0.7$ | $13.2 \pm 3.3$ | $8.4 \pm 0.6$ |
| 800 | $9.6 \pm 1.2$ | $2.9 \pm 0.1$ | $1.6 \pm 0.2$ | $1.7 \pm 0.4$ |
| 1000 | $9.5 \pm 0.5$ | $2.8 \pm 0.1$ | $1.9 \pm 0.1$ | $2.3 \pm 0.3$ |

sintering and densification. During cooling, a marked $E$ increase up to roughly a constant value (~96–100 GPa) was also observed, which is related to the material's stiffening. It can be noticed that such castables showed more significant rigidity gain during the beginning of the cooling cycles than the M–4HA–S (Fig. 6c). Most likely, this behavior is associated to the higher liquid amount expected to be formed for the CAC-bonded sintering additive-containing castables. Therefore, when the temperature decreased, the higher liquid viscosity resulted in these $E$ values changes. For the 2nd, 3rd heating cycles of the dried samples and the 1st cycle of the pre-fired ones, M–4CAC–S and M–2CAC–2HA–S kept their enhanced performance presenting some elastic modulus changes only in the 700–1000 °C temperature range due to the structure softening on heating or hardening on cooling (Fig. 6b and d).

When only hydratable alumina was used as the binder source, a continuous and steeper $E$ increase was observed between 700 and 1000 °C during the 1st heating treatment of the dried M–4HA–S castable, indicating that some phase transformations (i.e., formation of aluminum-borates, as shown in Fig. 4b) should result in the material's sintering. The elastic modulus also varied at the beginning of the cooling step (changing from 74 to 89 GPa). Additionally, this composition showed the highest thermal stability, as the rigidity of the samples was kept in the range of 79–91 GPa throughout the evaluation of subsequent thermal cycles (Fig. 6c).

The *in situ* $E$ modulus measurements for the sintering additive-containing castables (dried samples) with a holding time of 5 h at 1000 °C indicated that there is a substantial increase in the rigidity of the refractories in their first heating treatment, but few changes in their behavior could be detected during the dwell time (Fig. 7). All materials showed similar final elastic modulus (~98 GPa).

In order to analyze the stability of the designed castables after cyclical thermal shocks (0–8 cycles with $\Delta T$~800 °C, which is the working temperature of the refractories applied in FCCU), some additional elastic modulus measurements were carried out at room temperature. According to Fig. 8, besides the high mechanical performance attained for the M–2CAC–2HA–S and M–4HA–S castables at 800 °C and/or 1000 °C (Fig. 2a), those refractories showed almost no decrease in the elastic modulus as a function of the number of thermal cycles. Comparing the M–4CAC–S to the additive-free composition (M–4CAC), high initial elastic modulus and a continuous decrease in the $E$ values for this former were observed.

In general, it is accepted that strong materials result in catastrophic thermal shock failures owing to their ability to store high elastic energy [4]. The elastic strain stored energy is described by the following expression: $((1/2)(\sigma_f^2/E))$.

Both castables (M–4CAC–S and M–4HA–S) displayed similar initial $E$ values ($94.6 \pm 8.1$ GPa for the CAC-bonded material and $87.7 \pm 2.8$ GPa for the HA-bonded one) in the beginning of the thermal shock tests (0 cycle). However, considering that the M–4CAC–S samples presented higher HMOR values at 800 °C ($40.4 \pm 3.4$ MPa) than the M–HA–S ($16.3 \pm 0.9$ MPa) ones, it can be concluded that the former castable should store higher elastic energy levels in its structure, especially when such refractory is submitted to high thermal stress. Thus, the mechanical strength of the M–4CAC–S will play a major role to define the amount of the elastic strain stored energy that will be dissipated as surface energy, leading to flaws generation. This fact explains why the cement-bonded composition displayed better HMOR performance, but lower thermal shock resistance.

Therefore, based on the attained results, the blend of calcium aluminate cement and hydratable aluminas as the binders sources allowed the development of an improved refractory (M–2CAC–2HA–S) that showed high hot mechanical strength in a broader temperature range (800–1200 °C), low erosion resistance and high thermal stability.

## 4. Conclusions

The use of a boron-based sintering additive to speed up the refractory densification at lower temperatures seems to be a suitable alternative to develop novel compositions for the FCC petrochemical units. Despite the experimental difficulties for the evaluation of boron-containing systems, the *in situ* elastic modulus measurements indicated that above 600 °C some reactions should take place in the samples structure inducing sintering and densification. Quantitative XRD tests also showed that the main crystalline phases contained in the fired M–4CAC–S, M–4HA–S and M–2CAC–2HA–S materials were mullite, corundum and aluminum-borates (i.e $Al_4B_2O_9$ and $Al_{18}B_4O_{33}$) respectively. The formation of these boron-based phases in the presence of a transient liquid seems to be the main effect for the faster densification and enhanced performance of the designed compositions after firing at 800 °C, 1000 °C and 1200 °C.

Although the use of hydratable alumina+sintering additive in the designed M–4HA–S refractory resulted in good thermo-mechanical properties, this binder does not induce the

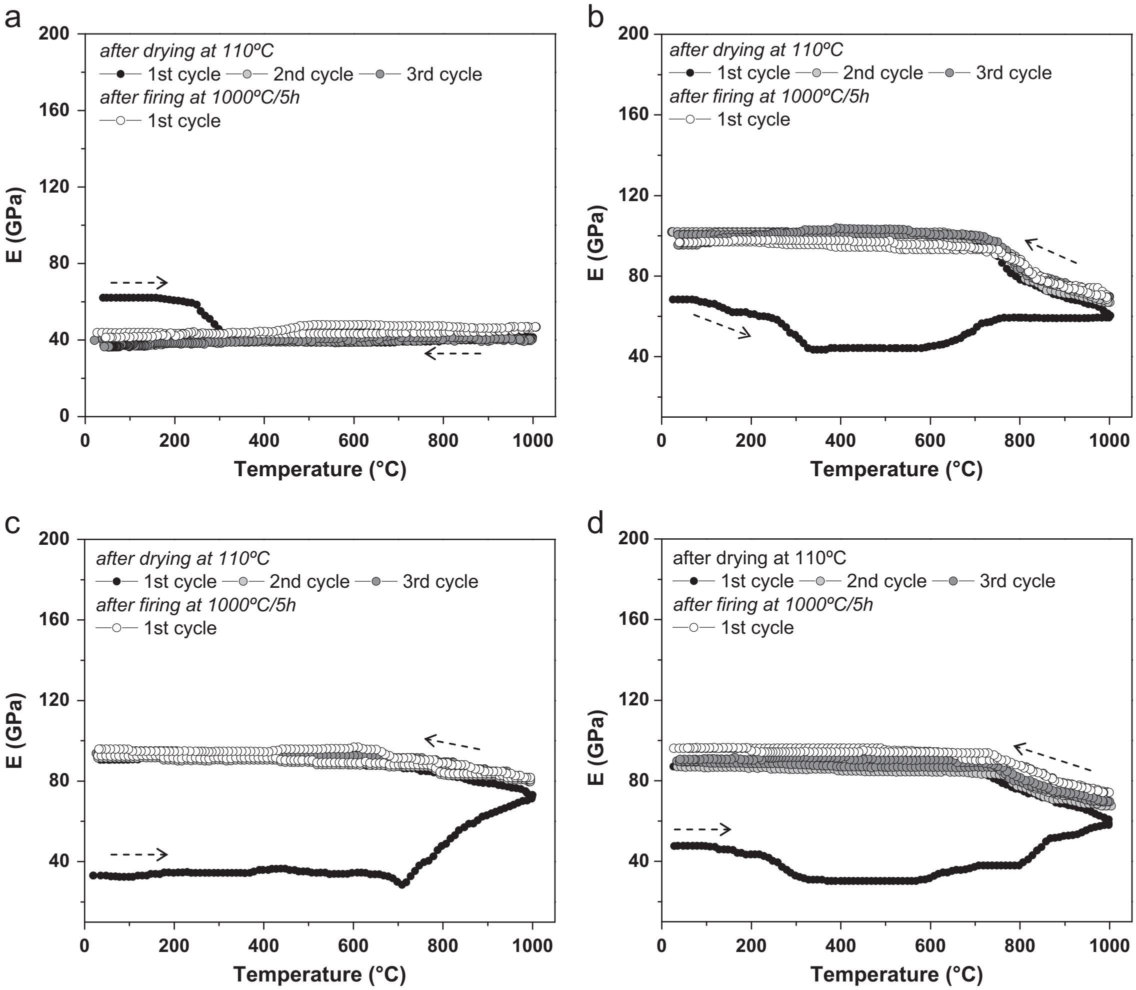

Fig. 6. *In situ* elastic modulus evolution as a function of the temperature (heating and cooling cycles up to 1000 °C): (a) M–4CAC, (b) M–4CAC–S, (c) M–4HA–S and (d) M–2CAC–2HA–S. The evaluated samples were previously cured at 50 °C for 24 h and dried at 110 °C for another 24 h, or even fired at 1000 °C for 5 h.

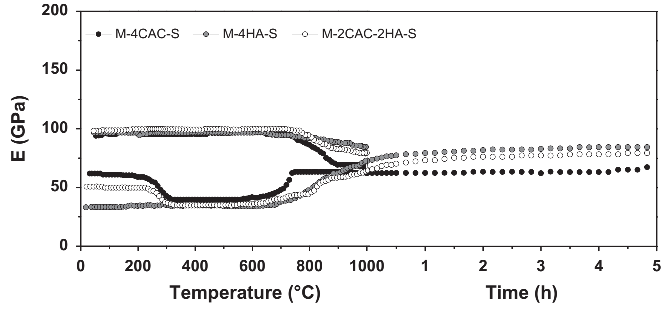

Fig. 7. *In situ* elastic modulus evolution as a function of the temperature and time. The evaluated samples were previously cured at 50 °C for 24 h and dried at 110 °C for another 24 h.

formation of strong bonds after firing the material at intermediate temperature (600 °C and 800 °C), leading to lower hot mechanical strength levels. The combination of calcium aluminate cement and hydratable alumina proved to be the best option for the development of high performance mullite-based refractory, as it resulted in a remarkable hot mechanical strength, thermal shock and erosion resistance with high refractoriness and *E* values in a broader temperature range (600–1200 °C). Therefore, not only the selection of a suitable sintering additive, but also the use of a single or a blend of binders should be considered in order to attain engineered compositions for the petrochemical field.

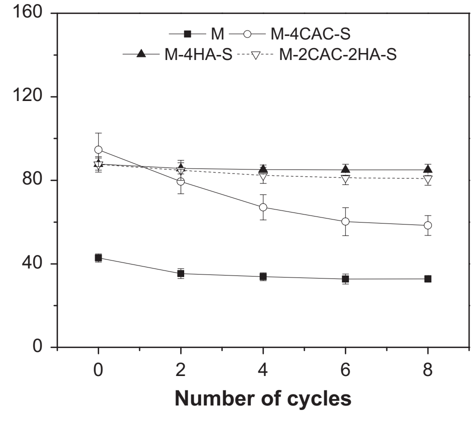

Fig. 8. Elastic modulus values as a function of thermal shock cycles ($\Delta T = 800$ °C).

## Acknowledgments

The authors would like to thank FIPAI, CNPq and Petrobras for supporting this work.

## References

[1] I.R. Oliveira, V.C. Pandolfelli, Chemical additives and their behavior on the refractory castable processing and properties, Refractories Applications and News 14 (1) (2009) 9–16.

[2] I.R. Oliveira, V.C. Pandolfelli, Castable matrix, additives and their role on hydraulic binder hydration, Ceramics International 35 (2009) 1453–1460.

[3] M.A.L. Braulio, G.G. Morbioli, J. Medeiros, J.B. Gallo, V.C. Pandolfelli, Nano-bonded wide temperature range designed refractory castables, Journal of the American Ceramic Society 95 (3) (2012) 1100–1104.

[4] A.P. Luz, T. Santos Jr., J. Medeiros, V.C. Pandolfelli, Thermal shock damage evaluation of refractory castables via hot elastic modulus measurements, Ceramics International 39 (2013) 6189–6197.

[5] P. Pena, A.H. de Aza, Cementos de aluminatos cálcicos. Constitución, características y aplicaciones, in: C. Baudin (Ed.), Refractarios Monolíticos, Sociedad Espanola de Cerámica y Vidrio, Madrid (Spain), 1999, pp. 85–106.

[6] C. Parr, F. Simonin, B. Touzo, C. Wohrmeyer, B. Valdelievre, A. Namba, The impact of calcium aluminate cement hydration upon the properties of refractory castables, In Proceedings TARJ Meeting (2004) 1–17.

[7] J.E. Kopanda, G. MacZura, Production processes, properties, and applications for calcium aluminate cements, in: L.D. Hart (Ed.), Alumina Chemicals Science and Tecnology Handbook, American Ceramic Society, Westerville (Ohio–USA), 1990, pp. 171–183.

[8] F.A. Cardoso, D.M.M. Innocentini, M.M. Akiyoshi, V.C. Pandolfelli, Effect of curing time on the properties of CAC bonded refractory castables, Journal of the European Ceramic Society 24 (2003) 2073–2078.

[9] J.A. Souza, in: Numerical simulation and thermodynamic optimization of risers for fluid catalytic cracking in fluidized bed for the maximum production of fuels (Ph.D. thesis), Universidade Federal do Paraná, Brazil 1–45 (in Portuguese).

[10] R. Salomão, M.R. Ismael, V.C. Pandolfelli, Hydraulic binders for refractory castables: mixing, curing and drying, CFI—Ceramic Forum International 84 (2007) E103–E108.

[11] M. Nouri-Khezrabad, M.A.L. Braulio, V.C. Pandolfelli, F. Golestani-Fard, H.R. Rezaie, Nano-bonded refractory castables, Ceramics International 39 (2013) 3479–3497.

[12] W. Ma, P.W. Brown, Mechanisms of reaction of hydratable aluminas, Journal of American Ceramic Society 82 (2) (1999) 453–456.

[13] R. Lorenz, G. Buchel, A. Buhr, J.M. Aroni, R.P. Racher, Improved workability of calcia-free alumina binder Alphabond for non-cement castables, in: Proceedings of the 47th International Colloquium on Refractories, Aachen, 2004, pp. 67–71.

[14] R.P. Racher, R. Kockegey, G. Buchel, A. Buhr, D. Gierisch, Improvement in workability behavior of calcia-free hydratable alumina binders. in: Proceedings of the UNITECR'05, Orlando, 2005, pp. 402–407.

[15] R.G. Pileggi, F.T. Ramal Jr., A.E.M. Paiva, V.C. Pandolfelli, High performance refractory castables: particle size design, Refractory Applications and News 8 (2003) 17–21.

[16] R.G. Pileggi, A. Studart, V.C. Pandolfelli, J. Gallo, How mixing affects the rheology of refractory castables—Part I, American Ceramic Society Bulletin 80 (2001) 27–31.

[17] G. Pickett, Equations for computing elastic constants from flexural and torsional resonant frequencies of vibration of prisms and cylinders, Proc. Am. Soc. Testing Mater. 45 (1945) 846-865.

[18] V. Swamy, I. Jung, S.A. Decterov, Thermodynamic modeling of the $Al_2O_3$–$B_2O_3$–$SiO_2$ system, Journal of Non-Crystalline Solids 355 (2009) 1679–1686.

[19] U.L. Schafer, H.I. Kuzel, Neues Jahrbuch für Mineralogie Monatshefte 4–5 (1967) 131.

[20] Slag Atlas, 2nd Edition, Dusseldorf: Verlag Stahleisen GmbH, 1995, p. 99.

[21] K.H. Kim, F.A. Hummel, Studies in lithium oxide systems: XII, $Li_2O_3$–$B_2O_3$–$Al_2O_3$, Journal of the American Ceramic Society 45 (10) (1962) 487–489.

[22] P.J. Gielisse, W.R. Foster, The system $Al_2O_3$–$B_2O_3$, Nature 195 (7) (1962) 69–70.

[23] V.A. Sokolov, M.D. Gasparyan, Synthesis and properties of fusion-cast refractories in the $Al_2O_3$–$B_2O_3$ system, Refractories and Industrial Ceramics 45 (3) (2004) 177–180.